



ISSN: 2319-5967

ISO 9001:2008 Certified

International Journal of Engineering Science and Innovative Technology (IJESIT)

Volume 3, Issue 5, September 2014

# Prediction of Residual Stress and Welding Deformation in Butt-weld Joint for Different Clamped Position on the Plates

Reenal Ritesh Chand, Ill Soo Kim, Qian Qian Wu, Bong yong Kang and JiYeon Shim

*Abstract—In this study, the three-dimensional moving distributed heat source model based on Goldak's double-ellipsoid heat flux distribution is implemented in Finite Element (FE) simulation for the GMA welding process. The thermal elastic-plastic analysis using FEM (Finite Element methods) has been carried out to analyze the thermo-mechanical behaviors and evaluate the residual stresses and welding deflection for butt joint plate, while assigning restrains (clamped) at the different position on the plate. Four different cases of simulation are being carried out; in each case that the plate is clamped at different positions. The temperature distributions, fusion and heat affected zones as well as residual stress and deflection for different cases is obtained and compared. From the compared results, the best case which has low deflection and residual stress is as the plate is clamped at two positions. The calculated results from FEM have been employed to verify that the welding deformation and residual is dependent on the different restrained position in the thin mild steel butt-welded joint.*

**Index Terms—Elastic-Plastic Analysis, Finite Element Simulation, Residual Stresses, Restraints, Welding Distortion**

## I. INTRODUCTION

Welding is a very important manufacturing technology which can be applied to almost every application that includes car, bicycles, shipbuilding and airplanes. A localized fusion zone is generated in the weld joint because of the high heat input from the arc and then non-uniform temperature distribution is induced due to the heat conduction. This results in non-linear plastic deformation and residual stress on the welded part. Welding deflection and residual stress often occurs in thin plate welded structures due to the relatively low stiffness which cause problems not only in the assembling process but also in the final product quality [1-4]. The residual stress promotes brittle fracture and corrosion cracking, reduce the buckling strength and fatigue life. The welding deformation often results in dimensional inaccuracies during product assembly and cost increase of the product [2]. In practical manufacturing process, it is impossible for experimental technique to obtain exert residual stress and deflection distribution in weld structure. Therefore, computational prediction of residual stress and welding deformation is critically important.

Many experimental and numerical analyses have been conducted to predict the temperature history, residual stress and welding distortion for single-pass welding [1-17]. However, there exists no complete mathematical model describing the prediction of residual stress and welding deformation in 4.5mm thin plate butt weld structures, especially for those structures which are restrained at certain position during welding process. For instant, Choobiet. al [1] demonstrated the effect of clamping on residual stress and distortion of less than 2mm thin butt welded plate by clamping the plate during welding process and releasing after cooling to ambient temperature has significant effect on the distortion of the plate. In other researches, Deng et. al [3] developed a 3D, thermo-elastic-plastic, large deformation FE to simulate the welding temperature field, residual stress and welding distortion in a low carbon steel butt-welded joint with 1mm thickness using a double ellipsoidal heat source distribution. It is shown that the numerical result calculated by the thermo-elastic-plastic, large deformation FE model was in a good agreement with the measurement. Deng [4] developed a sequentially coupled thermal, metallurgical, mechanical 3D finite element model to investigate the effects of solid-state phase transformation on welding residual stress and distortion in low carbon and medium carbon steels for the TIG arc welding. The elastic FEM with considering large deformation can be used to predict precisely welding deformation in the thin plate weld joint. Qureshet. al [5] conducted a parametric studies for the effects of a critical geometric parameter, that is, tack weld on the corresponding residual stress fields in circumferentially welded thin-walled cylinders. Tack welds offer a considerable resistance to the shrinkage and the orientation, and size of tacks can alter altogether the stress patterns within the weldments. Nguyen et al. [6] derived the analytical solutions for the transient temperature field of the semi-infinite body with conduction only consideration



ISSN: 2319-5967

ISO 9001:2008 Certified

International Journal of Engineering Science and Innovative Technology (IJESIT)

Volume 3, Issue 5, September 2014

subjected to 3D power density moving heat sources such as semi-ellipsoidal and double ellipsoidal heat sources. The solution has been obtained by integrating the instant point heat source throughout the volume of the heat source.

Even if the situation has greatly altered with the advent of increasing computer efficiency and better understanding of the physics of welding, only two papers were found as shown by Wang et. al [16] and Han et. al [17]. Wang et. al developed 2D thermal elastic-plastic finite element model based on ISM(Interactive Substructure method) to compute the welding deformation within practical time and discussed the relationship between welding heat parameters and welding deformation. Han et. al [17] presented a systematic finite element implementation of the constitutive equation of Leblond considering transformation plasticity. They strongly pointed out that phase transformation and the transformation plasticity have a significant effect on the residual stress of a welded structure. Although many engineers and researchers have made great effort how to control these incidents, they have still remained unresolved.

In this study, a mathematical model using FEM is considered to find the effect of clamping at different location on the residual stress and welding deformation in a 4.5mm thick butt-welded plate. A three-dimensional (3D) thermal elastic-plastic finite element analysis for GMA welding have been developed to numerically predict the residual stress and welding deformation on a butt-weld plate while being restrained at different locations. Four different cases were studied as for every case the plate is clamped at different location. The simulated results are compared with experimental results to find the best case.

## II. DEVELOPMENT OF WELDING SIMULATION MODEL

The numerical algorithm is employed in this study to calculate the residual stress and welding deformation due to GMA welding as shown in Fig. 1. Since the GMA welding process is a coupled thermo-mechanical phenomenon, structural field are dependent on the thermal field whereas, structural field have very weak influence on the thermal fields. Thus this coupled welding phenomenon can be split into thermal analysis followed by structural analysis.

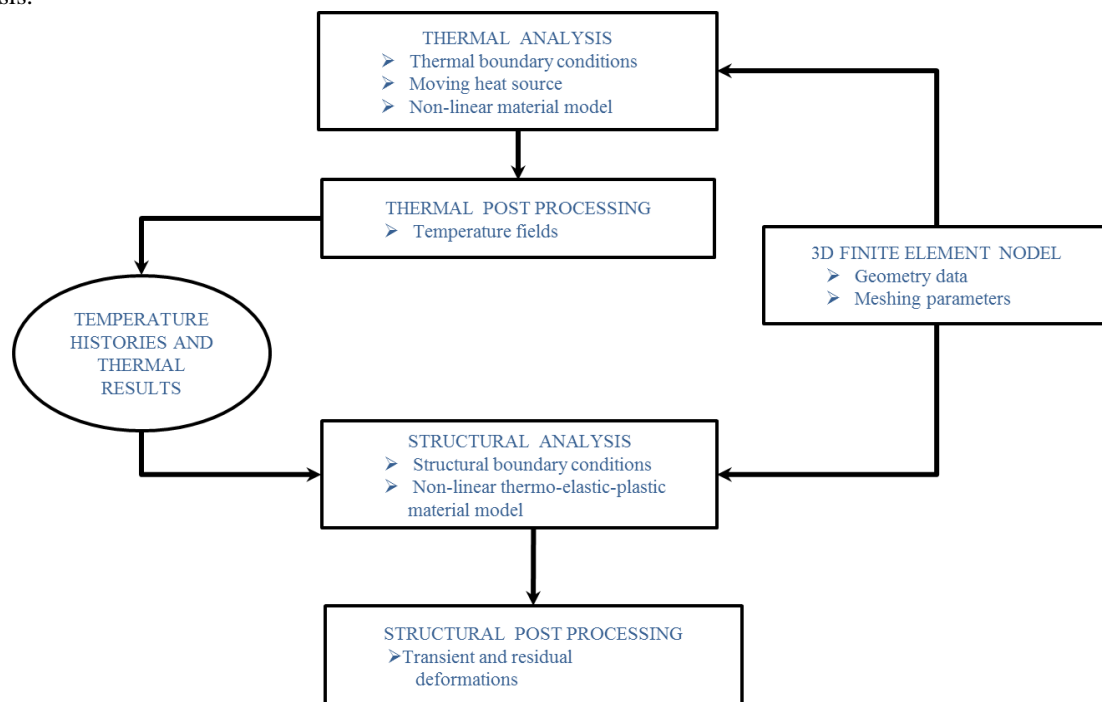


Fig. 1 Flowchart of numerical analysis for residual stress and welding deformation

### A. FE Model

A 3D FE model for 4.5mm thick butt-welded plate is developed in ANSYS software as shown in Fig. 2. The element type in thermal analysis is SOLID 70 (linear 8-node brick element with one degree of freedom, i.e.

temperature at each node). In mechanical analysis, SOLID 45 (linear 8-node brick element with three degree of freedom at each node, translations in the nodal X, Y, and Z direction) is employed. The boundary condition is the constraints applied to present the clamping at different position for each case illustrated below in Table 1 and each clamped position is indicated with respect to Fig. 2. Also the case, plate is clamped to have degree of freedom fixed x, y, z direction.

**Table 1. Case from the different clamped position**

Case number	Clamped edge
1	mid
2	1, 2, 3, 4
3	1, 2, 3,
4	2, 3

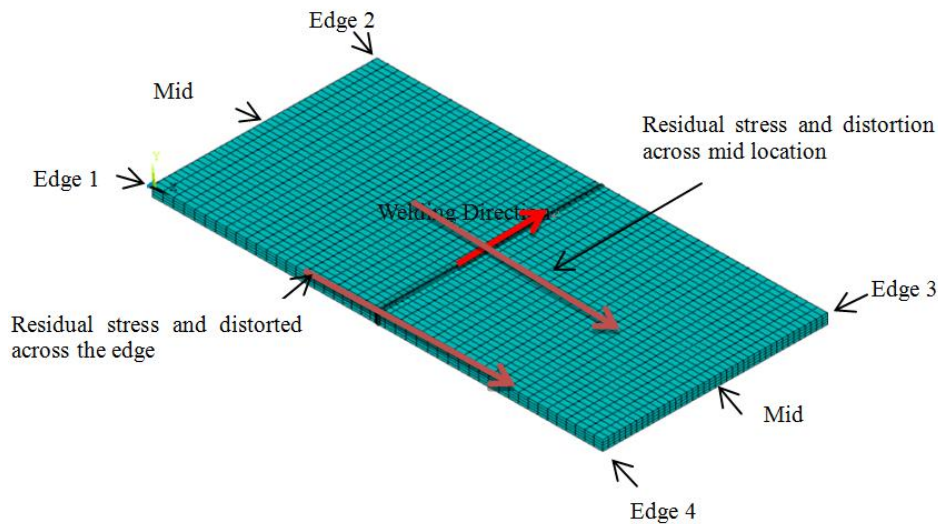


**Fig. 2 Finite element model for butt weld**

**B. Heat source and thermal analysis**

In the present, an analysis is represented with the temporal temperature distribution  $T(x, y, z, t)$  during GMA welding process and satisfied the following differential governing equation for 3D heat conduction by the following equation;

$$\rho c_R \frac{\partial T}{\partial t}(x, y, z, t) = -\nabla \cdot q(x, y, z, t) + Q(x, y, z, t) \quad (1)$$

Where  $\rho$  is the density of the material ( $\text{kg/m}^3$ ),  $c_R$  is the specific heat capacity ( $\text{J/g}^\circ\text{C}$ ),  $T$  is the temperature ( $^\circ\text{C}$ ),  $q$  is the heat flux vector ( $\text{W/m}^2$ ),  $Q$  is the internal heat generation rate ( $\text{W}$ ),  $x$ ,  $y$  and  $z$  are the coordinates in the reference system (m),  $t$  is the time (s) and  $\nabla$  is the gradient operator.

The non-linear isotropic Fourier's law is used to relate the heat flux vector to the thermal gradients;

$$q = -k \nabla T \quad (2)$$

Where  $k$  is the temperature-dependent thermal conductivity.

In representation of GMA welding process, the most widely acceptable double heat source model, presented by Goldak, is being used for the FE modeling [7]. The model gives the Gaussian distribution for the butt welding and

has excellent features of power and density distribution control in weld pool and HAZ(Heat Affected Zone) as shown in Fig. 3.

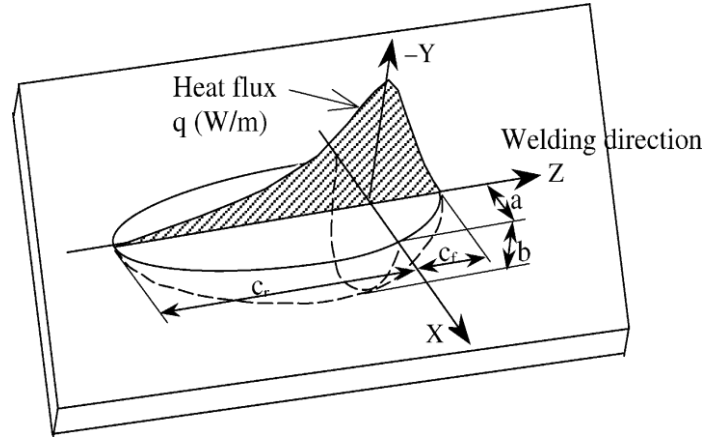


Fig. 3 Double ellipsoid heat source model

The Goldak's heat distributions are expressed by the following equations:

$$q_f(x, y, \xi) = \frac{6\sqrt{3}f_f Q}{abc_f \pi \sqrt{\pi}} e^{-\frac{3x^2}{a^2}} e^{-\frac{3y^2}{b^2}} e^{-\frac{3\xi^2}{c_f^2}} \quad (3)$$

$$q_r(x, y, \xi) = \frac{6\sqrt{3}f_r Q}{abc_r \pi \sqrt{\pi}} e^{-\frac{3x^2}{a^2}} e^{-\frac{3y^2}{b^2}} e^{-\frac{3\xi^2}{c_r^2}} \quad (4)$$

In where  $x$ ,  $y$ ,  $\xi$  are the local coordinates of the double ellipsoid model aligned with the welded pipe,  $f_f$  and  $f_r$  are parameters which give the fraction of the heat deposited in the front and the rear parts respectively.  $Q$  is the power of the welding heat source. Also,  $a$ ,  $b$ ,  $c_f$ ,  $c_r$  are related to the characteristics of the welding heat source.

The thermal boundary conditions include the radiation and convection to the environment from all the exposed surfaces, except the symmetry surface. Heat losses occur from the material surface through both convection and radiation. Radiation losses are dominating for higher temperatures near the weld zone, and convection losses are significant for low temperatures away from the weld line. From all heat dissipating surfaces, the heat lost is calculated [5].

$$h_{loss} = q_{convection} + q_{radiation} \quad (5)$$

$$q_{loss} = h_{total} xA (T - T_{amb}) \quad (6)$$

In which,  $A$  is the surface area,  $T$  is current temperature at the cylinder surface,  $T_{amb}$  is the ambient temperature and  $h_{total}$  is combined convection and radiation heat transfer coefficient.

$$h_{total} = [h_{convection} + \epsilon_{em} \sigma_{bol} (T - T_{amb})(T^2 + T_{amb}^2)] \quad (7)$$

The contribution of the transient temperature field and also temperature-dependent thermo-physical properties are used in simulation as shown in Fig. 4. The heat conduction problem has been solved using heat transfer analysis to obtain temperature histories.



ISSN: 2319-5967

ISO 9001:2008 Certified

International Journal of Engineering Science and Innovative Technology (IJESIT)  
Volume 3, Issue 5, September 2014

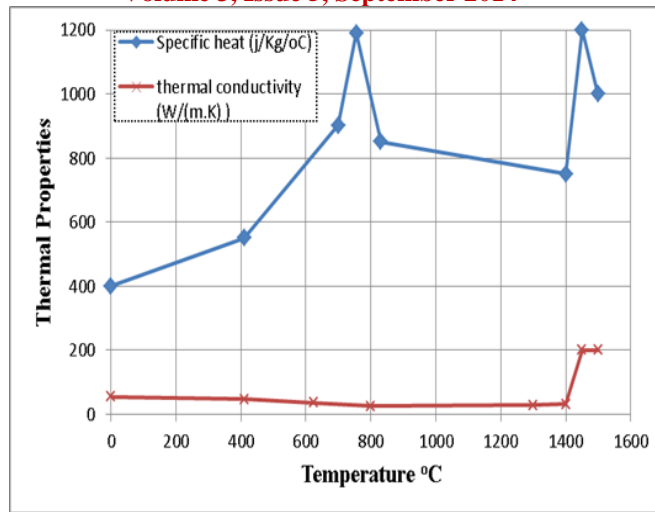


Fig. 4 Thermo-physical properties of mild steel as a function of temperature

Furthermore, the welding parameter of moving heat source for thermal simulation used in this study is listed in Table 2. The welding parameter is constant in all the cases in order to determine the effect of restrains during GMA welding process.

Table 2 Welding parameters employed for the study

Welding process parameter	Value
Welding voltage, V (volt)	25
Welding current, I (amperes)	200
Welding speed, v (mm/s)	4.8
Heat source efficiency, $\eta$ (%)	75

### C. Mechanical Simulation

For the mechanical analysis, the same FEM employed in the thermal analysis is employed in mechanical expect element type and boundary condition to simulate stress and strain fields for GMA welding process. The temperature history of each node from the preceding thermal analysis is input as the node load with temperature dependent mechanical properties shown in Fig. 5. In thermal-elastic-plastic constitutive models, total strains  $\epsilon^{total}$  rate are compose of elastic  $\epsilon^e$ , plastic strain  $\epsilon^p$  due to rate independent plasticity, thermal strain  $\epsilon^{th}$  consisting of thermal expansion.

$$\epsilon^{total} = \epsilon^e + \epsilon^p + \epsilon^{th} \quad (8)$$

The elastic strain is modeled using the isotropic Hook's law with temperature-dependent Young's modulus and Poisson's ratio. For the plastic strain component, a plastic model is employed with the following feature: the Von Mises yield surface and temperature-dependent material properties. A bi-linear kinematic hardening model (Von Mises yield criterion with associated flow rule, kinematic hardening rule and bi-linear kinematic hardening material) as shown below.

$$\sigma_v = \sqrt{\frac{1}{2}[(\sigma_1 - \sigma_2)^2 + (\sigma_2 - \sigma_3)^2 + (\sigma_3 - \sigma_1)^2]} \quad (9)$$

For the plastic strain, a rate-independent plastic model is employed with the following features: the Von Mises yield surface, temperature-dependent mechanical properties, and linear kinematic hardening model. Kinematic hardening is taken into account an important feature because material points typically go through both loading and unloading in course of the GMA welding process.

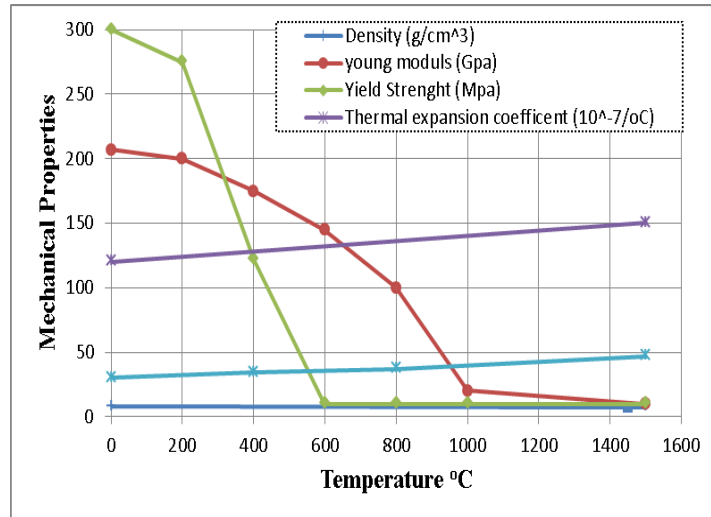


Fig. 5 Thermo-mechanical properties of mild steel as a function of temperature

### III. EXPERIMENTAL VALIDATIONS

The experiment has been conducted to validate the temperature distributions for all cases of numerical analysis. For experiment, a single pass GMA butt-welding is performed on a thin SM490 steel plate with dimensions of 200 x 100 x 4.5mm. The welding parameter is chosen as same for FE analysis. Fig. 6 shows the experiment setup for butt-welded joint.

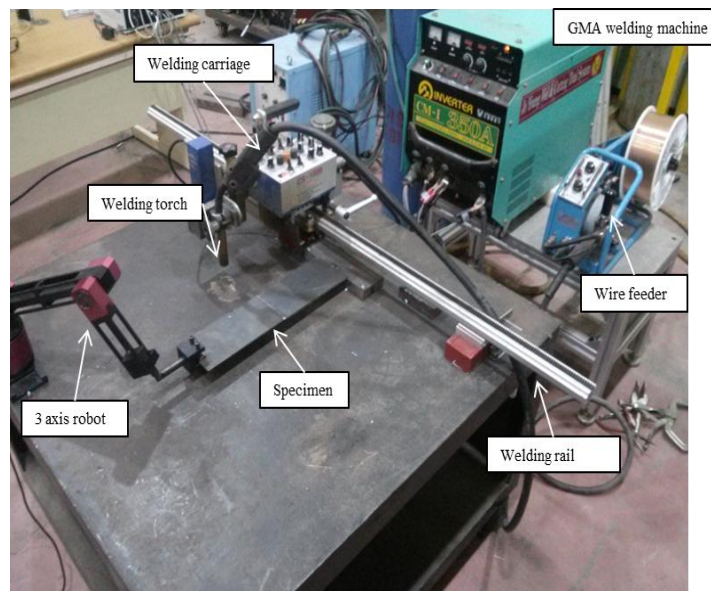


Fig. 6 Experiment setup of butt-welded joint

The temperature distributions during GMA welding process have been captured and measured using the thermal imagers with IR-Fusion. Once the IR captured image is viewed in smart-view software, 3D temperature distributions have graphically been plotted.

IV. RESULTS AND DISCUSSION

Fig. 7 depicts the temperature distribution in comparison with the measured and calculated results with respect to the distance across the center of weld plate respectively. The temperature distributions for the plate are presented after the peak temperature at plate is cooled down to about 200°C and the peak temperature during the GMA welding process at the top weld pool is noted to about 1500°C. It is noted from the Fig. 7 that the experimental value is good agreement with the numerical results computed the developed thermal model.

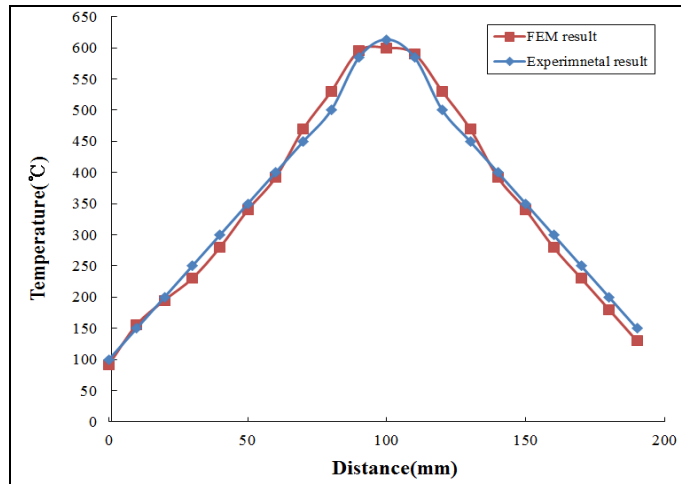


Fig. 7. Comparison of the measured and calculated temperature distributions

Fig. 8 shows the temperature histories of FZ (Fusion Zone) and HAZ (Heat Affect Zone) at the top and bottom surface at mid-section on the plate. The figure indicates that the temperature distributions of FZ and HAZ is not the same at the top and bottom surfaces, due to the plate thickness that results in uneven temperature distributions from top to bottom surface of the plate. Fig 9 shows the temperature distributions HAZ and FZ, both experimental and FEM indicate similar temperature distribution pattern and value. The distance from the weld center line and measured position is about 2.5mm whereas plate thickness is 4.5mm. Compared to the past research [10], 1mm thin weld plate showed no significant temperature gradient between top and bottom surface of the plate [1]. Fig. 9(a) and (b) shows FEM and experimental temperature for the 4.5mm thick butt welded plate, respectively.

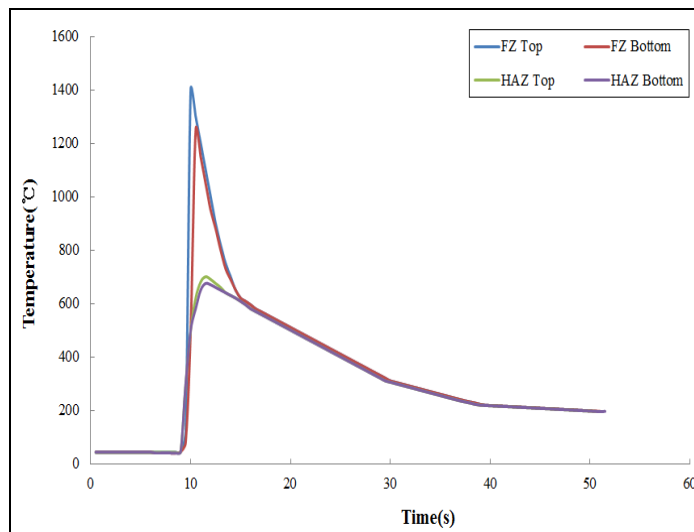
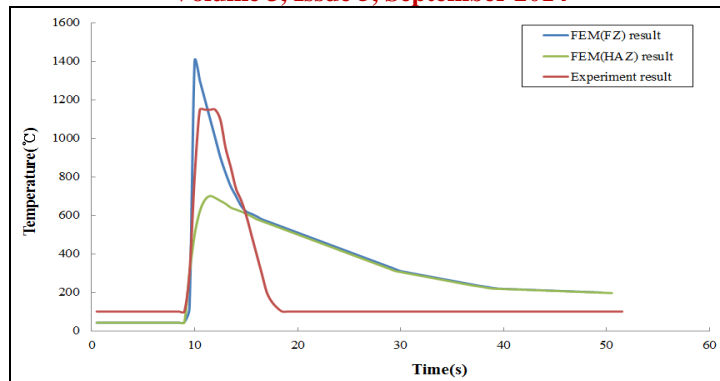
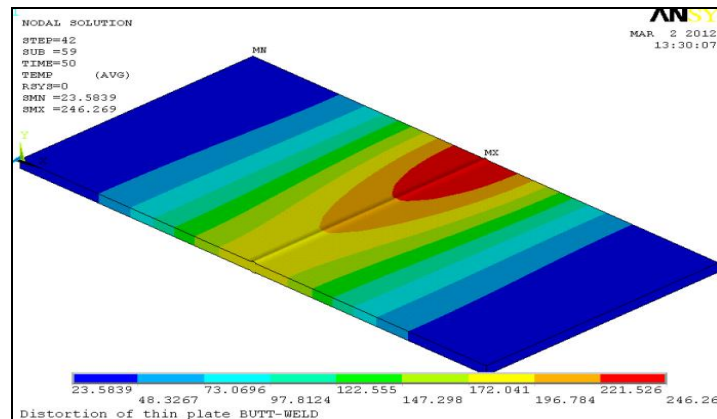


Fig. 8. Comparison of FZ with HAZ at top and bottom surface



(a) Comparison of the measured and calculated temperature distributions at top surface



(b) FEM temperature fields

Fig. 9. Comparison of FEM and experimental temperature fields on the plate for GMA welding

Fig. 10 shows the residual stress distribution with respect to the distance across mid-way of the welded plate. The residual stress distribution for all cases is similar in pattern except for case 1, and in all cases the plate is under tensile stress. In case 1, the distribution of residual stress at both plates clamped position is about 263MPa when the plate is clamped at the mid positions, but as approached towards welding region the residual stress is decreased rapidly and comes below 10MPa. In case 2, where all four edges are clamped, the residual stress at the edge of the mid location is about 80MPa, but as moved towards the welding region the residual stress increases to 90MPa and at actual area the residual stress drops to about 30MPa. For case 3 and 4 the stress distribution is similar as case 2 only residual stress magnitudes are different as indicated in fig.10.

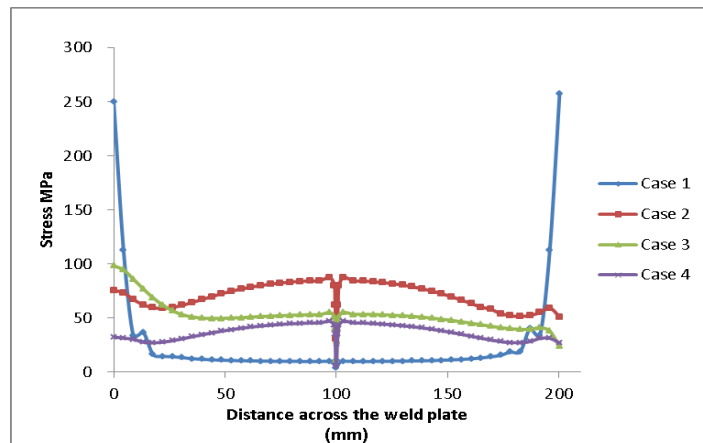


Fig. 10 Comparison of residual stress distribution across mid-way of the plate



Fig. 11 shows the residual stress distribution along the edge of the plate for all four cases. Residual stress distribution at the edge is different in each case and for all cases the plate is under tensile stress. For case 1, the residual stress at both the ends of plate is low about 5 MPa, but as moved towards the welding region the residual stress increases to about 100 MPa and at the actual welding area it decreases to about 50MPa. In case 2, the residual stress distribution around clamped locations is about 300MPa and it gradually decreases and becomes almost constant to about 10MPa as approach towards the welding regions. The residual stress distribution in case 3, a large residual stress is concentrated at the left side near edge 1 of the plate. Residual stress decreases from 300MPa significantly to a distance of about 10mm, then comes in between range of 10MPa to 1MPa as we approach the welding region moving towards the clamped edge 4 of the plate. The residual stress noted in case 4 is very low of about 1MPa, since the clamped position is on edge 2 and 3, giving less effect on residual stress along the edge 1 and 4. The effect of welding direction and welding speed is observed in Fig. 10 and 11; the magnitude of the stress is different since welding start edge has more cooling time compared to the welding ending edge of the plate.

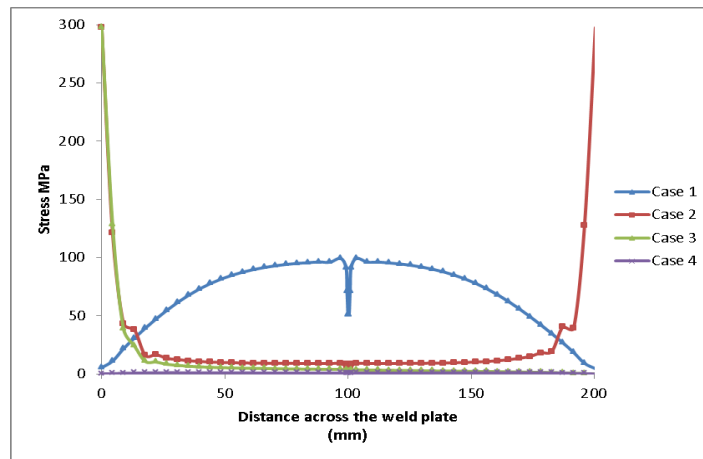


Fig. 11 Comparison of residual stress distribution along the edge of the plate

Fig. 12 shows comparison of deflection for different cases across mid-way of the plate. The results for case 1, shows that deflection at mid edge of the plate is zero, since the edges were clamped and the deflection gradually increases from the both mid ends of about 0.95mm at welding area.

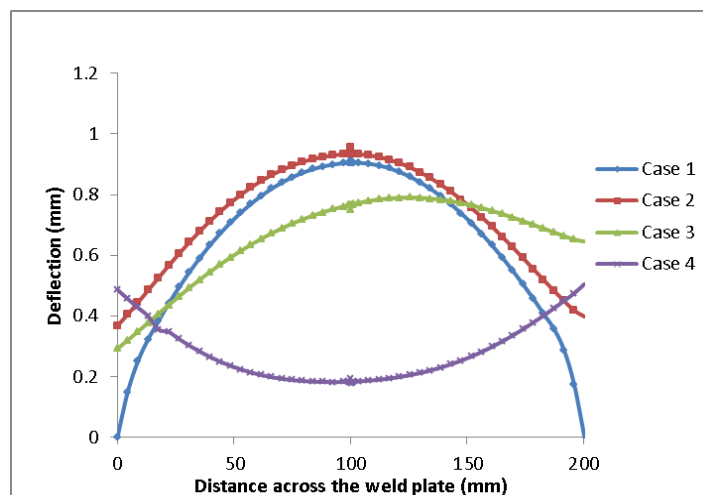


Fig. 12 Comparison of deflection distribution across mid-way of the plate

In case 2, similar pattern is noticed as in case 1, but both mid ends edge has deflection of about 0.5mm and gradually increases to the welding regions to about 1mm. In case 3 where the three edges are clamped, the deflection at the left side of plate is small about 0.3mm, but as moved towards the welding region it increases to about 0.8mm and at right side of the plate of about 0.65mm. The two edges at the left side of the plate are clamped,

giving less deflection at mid location compare to the right side of the plate where only one edge is restrained. In case 4 where two edges are clamped, the deflection along the plate is different from all the cases, deflection at both mid edges is about 0.5mm. The deflection decreases across the plate as welding region is approached from the both edges of plates and minimum deflection of about 0.2mm is noted around the welding area.

Fig. 13 shows the deflection along the side edges of the plate. The cases 1 and 4 have similar deflection distribution along the edges, where it has large deflection shown at end of the plate, and less deflection near the welding region. Whereas case 4 has large deflection of about 0.67mm near welding compared to case 1 which has 0.15mm. In case 2, there is no deflection at edges 1 and 4, since edge 1, 2, 3 and 4 edges are clamped, but along the plate, maximum deflection is noted at welding region of about 1mm. In case 3, deflection at right side plate was noted to about 1mm and deflection at the left side plate edge 1 is 0, the deflection increases as moved toward the welding region, since edge 1, 2 and 3 is clamped. The largest deflection is noted out of all case in case 2, both deflections on along the mid-way and along the edges of the plate found to be largest as shown in both the deflection graphs.

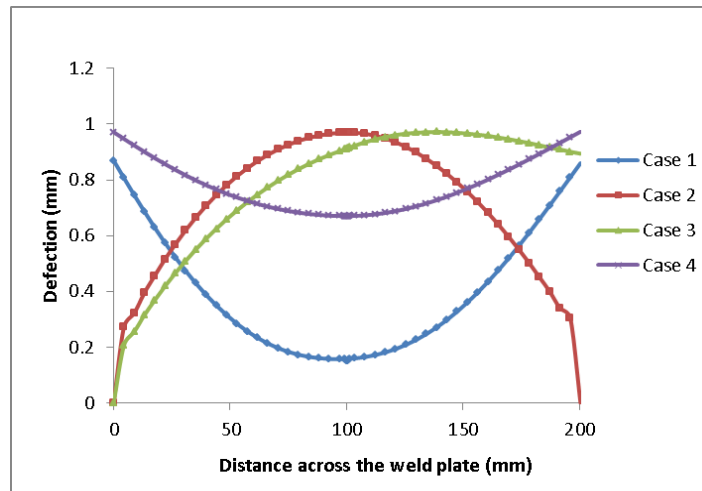


Fig. 13 Comparison of deflection distribution along the edge of the plate

The result shows that clamping or restraining the plate during welding process has large impact on residual stress and distortion. In previous, researches, Deng [4] and Han [17] investigate the effects of solid-state phase transformation on welding residual stress. In comparison to this study, one can depict the residual stress and distortion or deflection also dependent on the peak temperature and the restraining conditions. In comparison with different cases, cases 1 and 4 give the best results which have low residual stress and deflection across the plate.

## V. CONCLUSION

This study, investigates the effect of restraining (clamped) the mild steel plate at different position on residual stress and deflection in a computational simulation of welding process. Detailed three dimensional nonlinear thermal and thermo-mechanical analyses are performed using FE model for 4.5mm thick butt welding plate. According to the numerical analysis results, the following conclusion can be drawn.

- (1) Based on simulation results and past research paper [1], it can be known that there is a change in temperature gradient through the plate thickness as the plate thickness is increased in butt welding.
- (2) Comparing the residual stress and deflection for the different cases of 4.5mm thick butt welding process of mild steel, it is revealed that restraining the plate has a large effect on the distribution of residual stress and deflection. It could be generalized that factors such as residual stress, deflection and plate strain is mainly dependent on the peak temperature and restraining conditions that are applied on the plate.
- (3) The welding direction and welding speed has also some effect on residual stress, the large magnitude of stress is noted at the edges compared to across the mid-way of the plate, this is due to the start edge having more cooling time compared to the ending edge.



ISSN: 2319-5967

ISO 9001:2008 Certified

International Journal of Engineering Science and Innovative Technology (IJESIT)

Volume 3, Issue 5, September 2014

#### ACKNOWLEDGMENT

This research was financially supported by the Ministry of Education (MOE) and National Research Foundation of Korea (NRF) through the Human Resource Training Project for Regional Innovation (No. 2013H1B8A2032082 ).

#### REFERENCES

- [1] M. Seyyedian Choobi, M. Haghpanahi and M. Sedighi, "Investigation of the effect of clamping on residual stress and distortion in butt-welded plate," *Journal of Scientia Iranica Transaction B: Mechanical Engineering*, vol. 17, no. 5, pp. 387-394, 2010.
- [2] X.K. Zhu, and Y.J. Chao, "Effect of temperature-dependent material properties on welding simulation," *Journal of Computers and Structures*, vol. 80, pp. 967-976, 2002.
- [3] K. Deng and H. Murakawa, "Prediction of welding distortion and residual stress in a thin plate butt-welded joint," *Journal of Computational Material Science*, vol. 43, pp. 353-365, 2008.
- [4] D. Deng, "FEM prediction of welding residual stress and distortion in carbon steel considering phase transformation effect," *Journal of Materials & Design*, vol. 30, pp. 359-366, 2009.
- [5] E.M. Quresh, A.M. Malik and N.U. Dar, "Residual stress field due to varying tack welds orientation in circumferentially welded thin-walled cylinder," *Journal of Advance in Mechanical Engineering*, vol. 2009, pp. 1-9, 2009.
- [6] Nguyen, N. T., Ohta, A., Matsuoka, K., Suzuki, N. and Maeda, Y. "Analytical solutions for transient temperature of semi-infinite body subjected to 3-D moving heat sources," *Welding Journal Research Supplement*, pp. 265-274, 1999.
- [7] J. Goldak, A. Chakravarti and M. Bibby, "A new finite-element model for welding heat," *Journal of Metallurgical and Material, Transaction B*, vol. 15, pp. 299-305, 1984.
- [8] M.J. Attaeha and I. Sattari-Farl, "Study on welding temperature distribution in thin welded plates through experiment measurements and finite element simulation," *Materials Processing Technology*, vol. 211, pp. 688-694, 2011.
- [9] P. Duranton, J. Devaux, V. Robin, P. Gilles and J.M. Bergheau, "3D modeling of multipass welding of a 316L stainless steel pipe," *Journal of Materials Processing Technology*, vol. 153-154, pp. 457-463, 2004.
- [10] H.T. Lee and J.L. Wu, "The effects of peak temperature and cooling rate on the susceptibility to intergranular corrosion of alloy 690 by laser beam and gas tungsten arc welding," *Corrosion Science*, vol. 51, pp. 439-445, 2009.
- [11] C.H. Lee and K.H. Chang, "Three-dimensional finite element simulation of residual stresses in circumferential welds of steel pipe including pipe diameter effects," *Materials Science & Engineering A*, vol. 487, pp. 210-218, 2008.
- [12] F. Lu, S. Yao, S. Lou, and Y. Li, "Modeling and finite element analysis on GTAW arc and weld pool," *Computational Materials Science*, vol. 29, pp. 371-378, 2004.
- [13] N.T. Nguyen, A. Ohta, K. Matsuoka, N. Suzuki and Y. Maeda, "Analytical solutions for transient temperature of semi-infinite body subjected to 3-D moving heat sources," *Welding Journal Research Supplement*, pp. 265-274, 1999.
- [14] F. Vakili-Tahami and A.H.D. Sorkhabi, "Finite element analysis of thickness effect on the residual stress in butt-welded 2.25Cr1Mo steel plates," *Journal of Applied Science*, vol. 9, pp. 1331-1337, 2009.
- [15] T.T., Doan, T.Q, Vo and I.S., Kim, "Finite element predictions of residual stress and distortion," *11th Asia Pacific Industrial Engineering and Management System*, October 7-10; Melaka, Malaysia, 2010.
- [16] C., Heinze, C., Schwenk, M., Rethmeier, "Numerical calculation of residual stress development of multi-pass gas metal arc welding under a high restraint conditions," *J. Material and Design*, vol. 35, pp. 201-209, 2012.
- [17] Y.S. Han, K., Lee, M.S., Han, H., Chang, K, Choi, S., IM, "Finite element analysis of welding processes by way of hypoelasticity-based formulation," *Journal of Engineering Materials and Technology*, vol. 133, pp. 021103.1-021103.13, 2011.